3D Face Recognition with Asymptotic Cones based Principal Curvatures

Yinhang Tang[1], Xiang Sun[2], Di Huang[3], Jean-Marie Morvan[2,4], Yunhong Wang[3], Liming Chen[1]

[1]Université de Lyon, CNRS, Ecole Centrale de Lyon, LIRIS, Lyon, 69134, France

[2]King Abdullah University of Science and Technology, $V.C.C.$ Research Center, Thuwal 23955-6900, Saudi Arabia

[3]IRIP, School of Computer Science and Engineering, Beihang Universtiy, Beijing 100191, China

[4]Université de Lyon, CNRS, Université Claude Bernard Lyon 1, ICJ UMR 5208, Villeurbanne F-69622, France

germain.tang-yinhang@doctorant.ec-lyon.fr, xiang.sun@kaust.edu.sa, dhuang@buaa.edu.cn, morvan@math.univ-lyon1.fr, yhwang@buaa.edu.cn, liming.chen@ec-lyon.fr

Abstract

The classical curvatures of smooth surfaces (Gaussian, mean and principal curvatures) have been widely used in 3D face recognition (FR). However, facial surfaces resulting from 3D sensors are discrete meshes. In this paper, we present a general framework and define three principal curvatures on discrete surfaces for the purpose of 3D FR. These principal curvatures are derived from the construction of asymptotic cones associated to any Borel subset of the discrete surface. They describe the local geometry of the underlying mesh. First two of them correspond to the classical principal curvatures in the smooth case. We isolate the third principal curvature that carries out meaningful geometric shape information. The three principal curvatures in different Borel subsets scales give multi-scale local facial surface descriptors. We combine the proposed principal curvatures with the LNP-based facial descriptor and SRC for recognition. The identification and verification experiments demonstrate the practicability and accuracy of the third principal curvature and the fusion of multi-scale Borel subset descriptors on 3D face from FRGC v2.0.

1. Introduction

In the last few decades, Biometrics is extensively used in computer science as a form of human identification and access control. There exist different kinds of biometrics, such as fingerprint, iris, and face. Comparing to acquiring the fingerprint and iris data which are unrealistic or undesirable due to the problems of social acceptance [9], the face has its unique advantages for applications in scenario. Because of its natural, nonintrusive and contactless data collection mode [8], face recognition has developed rapidly. With the development of 3D information acquisition technology, it is convenient to collect 3D data and thus FR has attracted increasing attentions in recent years [18, 2].

Since 3D face sensors can accurately and sensitively capture the geometrical shape of the underlying 3D facial surfaces, designing a discriminating facial geometric surface feature is a critical issue in 3D face recognition. In general, the normal and the curvatures (*e.g.*, principal curvature, mean curvature and Gaussian curvature) are the most commonly used geometric features to describe the facial local surface. Maes *et al.* applied the mean curvature in DoG based scale space to detect salient vertices and then adopted histogram of shape index (calculated with maximal curvature and minimal curvature) in local regions to build the descriptor [13]. Kakadiaris *et al.* analyzed the normal map and geometry image by using a wavelet transform [10]. Szeptycki *et al.* adopted the mean curvature and the Gaussian curvature to locate the most salient facial feature points (*e.g.*, nose tip and two eye inner corners) [23]. Li *et al.* proposed Multiple salient vertices based Histograms of Multiple order surface differential Quantities computed in the neighborhood of salient vertices automatically using the histograms of shape index and gradients of shape index based on maximal and minimal curvatures through a 3D Gaussian scale space [11]. Tonchev *et al.* processed the curvature analysis and range image representation on the input point cloud [24]. Hwang *et al.* extended Gabor wavelet kernels by adding a spatial curvature term and adjusted the width of the Gaussian at the kernel for a low-resolution image [7]. These works proposed efficient facial surface features and achieved outstanding experiment results.

The related work presented above commonly utilized the principal curvatures (maximal curvature and minimal curvature), the mean curvature and Gaussian curvature defined on smooth surfaces. But the 3D face data used in the above works are usually recorded as triangle meshes. That is why, following [3, 4, 14], we introduce three eigenvalues, at each Borel subset, deriving from the generalized second funda-

mental measure.

Following the same ideas, we introduce the notion of *asymptotic cone* associated to a Borel subset B of $\mathbb{E}^3$ that generalizes the *asymptotic directions* defined at each point of a smooth surface [22, 21]. This method generates three principal curvatures $\lambda_1(B)$, $\lambda_2(B)$ and $\lambda_3(B)$ corresponding to the three eigenvalues of the quadratic form that defines the asymptotic cone. By extracting LNP local descriptors from the faces built by $\lambda_1(B)$, $\lambda_2(B)$, $\lambda_3(B)$ and testing the recognition performance in experiment, we highlight the descriptor based on $\lambda_3(B)$. This descriptor performs the discriminative power.

As a further step, we realize that different scales of Borel subsets give rise to different values of the principal curvatures. The combination of descriptors based on multi-scale Borel subsets improves the recognition performance.

The rest of this paper is organized as follows. Section 2 describes the construction of the asymptotic cones. Section 3 presents the multi-scale asymptotic cone based local feature descriptor. Section 4 shows the experimental results. Section 5 concludes the paper.

2. Asymptotic cone

The notion of asymptotic cones is first introduced in [22] and [21] to generalize the notion of asymptotic directions of any point on a smooth surface. In this section we will briefly summarize the construction of the asymptotic cones defined on smooth surfaces and triangle meshes.

2.1. The case of smooth surfaces in $\mathbb{E}^3$

First let us consider a smooth oriented surface W^2 embedded in the Euclidean space $\mathbb{E}^3$. Let ξ be a normal vector field compatible with the orientation. let h be the second fundamental form of W^2 in the direction of ξ. At each point m, we denote by λ_{1_m}, λ_{2_m} the principal curvatures of W^2, that is, the eigenvalues of h_m. We denote by G the Gaussian curvature of W^2, that is, the determinant of h and by H its mean curvature, that is, its trace. In an orthonormal frame of principal vectors (e_{1_m},e_{2_m}) at m (eigenvectors of h_m), the matrix of h_m is

$$\begin{pmatrix} \lambda_{1_m} & 0 \\ 0 & \lambda_{2_m} \end{pmatrix} \tag{1}$$

At each point $m \in W^2$ with negative Gaussian curvature, the *asymptotic cone* $\boldsymbol{C}_m$ is the union of two lines on the tangent plane T_mW^2 defined by $h_m(x,x) = 0$.

Let us define such a cone over any (compact) Borel subset B of $\mathbb{E}^3$. Let $T_{W^2}\mathbb{E}^3$ be the tangent bundle of $\mathbb{E}^3$ restricted to W^2. If x is any vector field on $T_{W^2}\mathbb{E}^3$, we build a signed measure $\Phi^x_{W^2}$ as follows: for any Borel subset B of $\mathbb{E}^3$, we put

$$\Phi^x_{W^2}(B) = \int_{B\cap W^2} h_m(pr_{T_mW^2}x, pr_{T_mW^2}x)dm \tag{2}$$

where $pr_{T_mW^2}$ denotes the orthogonal projection on T_mW^2 and dm the Lebesgue measure on $\mathbb{E}^3$. Let us now fix B and consider the map

$$x \to \Phi^x_{W^2}(B) \tag{3}$$

where x runs over the space of constant vector fields $\Xi(\mathbb{E}^3)|_{(W^2)}$. This map is a quadratic form on $\mathbb{E}^3$. It has three eigenvalues $\lambda_1(B)$, $\lambda_2(B)$, $\lambda_3(B)$ that we call the principal curvatures of B. The corresponding eigenvectors will be called the principal vectors of B, and the matrix of $\Phi^2_W(B)$ in this frame is

$$\begin{pmatrix} \lambda_1(B) & 0 & 0 \\ 0 & \lambda_2(B) & 0 \\ 0 & 0 & \lambda_3(B) \end{pmatrix} \tag{4}$$

We introduce also the isotropic cone associated to $\Phi^2_W(B)$:

$$\mathcal{C}^{W^2}_B = \{x \in \mathbb{E}^3; \Phi^x_{W^2}(B) = 0\} \tag{5}$$

We call it the *asymptotic cone* of B with respect to W^2.

To clarify the link of this construction with the classical pointwise one, let us suppose that B is reduced to a point $\{m\} \in W^2$.

If $y_m \in T_mW^2$, then

$$\Phi^y_{W^2}(\{m\}) = h_m(y_m, y_m) \tag{6}$$

If $z_m = \xi_m$, then

$$\Phi^z_{W^2}(\{m\}) = 0 \tag{7}$$

This implies that in the frame $(e_{1_m}, e_{2_m}, \xi_m)$, the matrix of $\Phi_{W^2}(\{m\})$ is

$$\begin{pmatrix} \lambda_{1_m} & 0 & 0 \\ 0 & \lambda_{2_m} & 0 \\ 0 & 0 & 0 \end{pmatrix} \tag{8}$$

Consequently, the asymptotic cone $\mathcal{C}^{W^2}_m$ is nothing but the cone spanned by the normal ξ_m and $\boldsymbol{C}_m$.

This point of view has some advantages: First, one can study the surface at different scales, by scaling the Borel sets which conduct to the multi-scale asymptotic cone based feature applied in this paper; second, we get three geometric invariants $\lambda_1(B), \lambda_2(B), \lambda_3(B)$ associated to each Borel set B instead of two; third, replacing functions by measures, we can defined asymptotic cones and principal curvatures on triangle meshes.

2.2. The case of triangulations

The following paragraph gives the equation of the asymptotic cone for a triangle mesh P^2 associated to any Borel subset in $\mathbb{E}^3$.

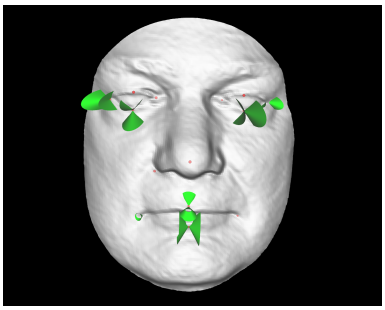

Figure 1. Asymptotic cones found around feature points (cones are colored in green and feature points are colored in red dots)

Let e be an edge of P^2. Let us denote by n_1 (resp. n_2) the unit oriented normal of face f_1 (resp. f_2) incident to e. Let e^+ (resp. e^-) be the oriented normalized vectors spanning the bisectors of n_1 and n_2 (so that (e^+, e^-, e) is a direct frame of $\mathbb{E}^3$.

For any Borel subset B and any vector x of $\mathbb{E}^3$, a directed computation [3, 4, 14, 22] gives

$$\Phi^x_{P^2}(B) = \sum_{e\in E} \frac{l(e\cap B)}{2}[(\angle(e) - sin\angle(e)) < x, e^+ >^2 + (\angle(e) + sin\angle(e)) < x, e^- >^2] \quad (9)$$

where E denotes the set of edges of P^2 and $\angle(e)$ is the signed angle between n_1 and n_2. It is positive if e is convex and negative otherwise.

Then the asymptotic cone $\mathcal{C}_B^{P^2}$ is defined by

$$\mathcal{C}_B^{P^2} = \{x \in \mathbb{E}^3 : \Phi^x_{p^2}(B) = 0\} \quad (10)$$

Remark that if $\angle(e)$ is small enough (this can happen for instance when P^2 approximates a smooth surface [14, 16, 15]), then $sin\angle(e)$ is close to $\angle(e)$ and we have a simpler expression

$$\Phi^x_{p^2}(B) \sim \sum_{e\in E} l(e\cap B)\angle(e) < x, e^- >^2 \quad (11)$$

Here we give some asymptotic cones found in some feature points on a 3D face model (in Fig.1). In some feature points, the generated asymptotic cones are virtual cones which can't be drawn in the figure. However their three eigenvalues will be used in the following descriptors.

3. Asymptotic cone based facial descriptor

The asymptotic cones based 3D face recognition method proposed in this paper could be separated into the following parts (shown in Fig.2): face preprocessing, face alignment, generating asymptotic cones based principal curvatures, creating the three curvature faces corresponding to each principal curvature, extracting LNP-based facial descriptor from the curvature faces, SRC matching and fusion.

3.1. Preprocessing and alignment

Data collection with 3D scanner is affected by the undesired noise which generates the spikes. The receptor in the 3D scanner fails to receive the reflection laser beam at certain point which produces the unexpected holes. Thus the spike removing and holes filling are necessary in the preprocessing.

In consideration of the accuracy of LNP-based facial descriptor, the Iterative Closest Point (ICP) is also applied to normalize the rotation of the 3D face data. Five landmarks (left eye inner corner, left eye outer corner, right eye inner corner, right eye outer corner, nose tip) of each face model are located following [23]. Based on the triangle of the two midpoints of inner corner and outer corner and the nose tip, we normalized the scale of face.

3.2. Asymptotic cone based principal curvature

Our purpose is to estimate the principal curvatures to describe the geometric properties of each vertex. As defined in section 2.2 , an approximated asymptotic cone is the set of solutions of the following equation:

$$\sum_{e\in E} l(e\cap B)\angle(e) < Z, e >^2 = 0 \quad (12)$$

Eq.12 is quadratic and can be written in the standard form as:

$$Z^t \times H \times Z + b^t \times Z + c = 0 \quad (13)$$

where H is a three-by-three matrix, b, c and Z are vectors in 3D.

From two equations above, we construct H:

$$H = \begin{pmatrix} H_{11} & H_{12} & H_{13} \\ H_{21} & H_{22} & H_{23} \\ H_{31} & H_{32} & H_{33} \end{pmatrix}$$

$$\begin{cases} H_{11} = \sum_{e\cap B} A_e e_x^2 \\ H_{22} = \sum_{e\cap B} A_e e_y^2 \\ H_{33} = \sum_{e\cap B} A_e e_z^2 \\ H_{12} = H_{21} = \sum_{e\cap B} A_e e_x e_y \\ H_{23} = H_{32} = \sum_{e\cap B} A_e e_y e_z \\ H_{31} = H_{13} = \sum_{e\cap B} A_e e_z e_x \end{cases} \quad (14)$$

where $A_e = l(e\cap B)\angle(e), e_x, e_y, e_z$ are the components of the unit vector parallel to the edge. Moreover l is the length and $\angle(e)$ represents the signed angle between the normals of the two oriented triangles incident to e.

Based on the definition of asymptotic cone, the first and second principal curvatures are estimated as maximal curvature and minimal curvature. However the third principal should also be considered.

For the convenience of the computation we take Borel subsets as balls centered at the vertices of the mesh.

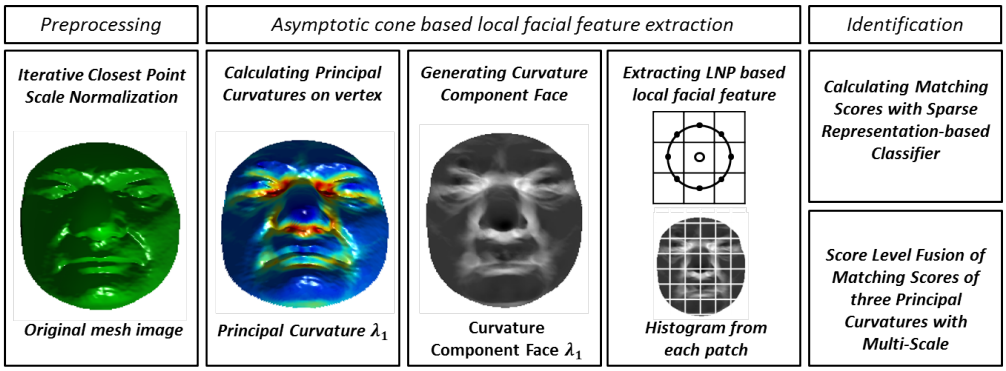

Figure 2. Overview of our proposed method

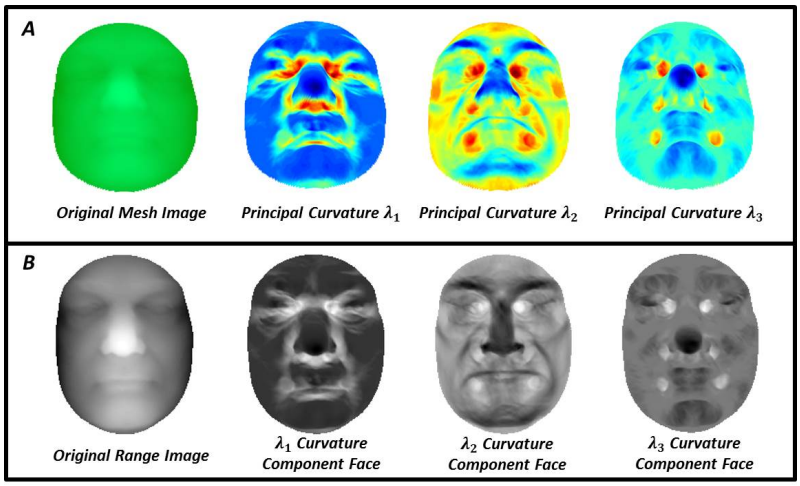

Figure 3. (A) Principal curvatures calculated on each vertex. The color presents the value of principal curvature; (B) Curvature Face generated from group A and principal curvature is normalized to 0-255.

Through changing the radius of the balls, the values of principal curvatures vary. Fig.3 (A) shows the three principal curvatures calculated on each vertex which present surface local geometric properties.

3.3. Generating curvature face

Considering that LNP-based local facial feature descriptor (in section 3.4) is usually extracted in range image, the principal curvatures of each vertex need to be presented in 2D image. For achieving this goal, the range image with resolution of 320×240 called *curvature face* is generated. The value of each pixel in curvature face relates the principal curvatures of its corresponding points in the mesh model. Obviously, we can't guarantee that each corresponding point locates on the vertex of the mesh model, therefore we apply the area based interpolation to estimate the value of the pixel in curvature face.

Here we suppose that the value of pixel p in curvature face is the one estimated. But its corresponding point P locates in the triangular surface patch $\triangle ABC$ (A, B and C are the vertices of mesh model). Thus the principal curvature of P is presented:

$$C_P = \frac{S_{\triangle PBC}}{S_{\triangle ABC}} C_A + \frac{S_{\triangle PCA}}{S_{\triangle ABC}} C_B + \frac{S_{\triangle PAB}}{S_{\triangle ABC}} C_C \quad (15)$$

where C_P, C_A, C_B and C_C are the principal curvatures of corresponding points, S is the triangular area.

The samples of three curvature faces are shown in Fig.3 (B). This figure clearly shows that each curvature face generated by the corresponding principal curvature contain more informative geometric information than its corresponding range image which looks quite smooth. Especially, the geometric shape details around the eye corners, mouth corners and cheek region are quite well highlighted.

3.4. Local Normal Patterns based descriptor

Once three curvature faces in mesh model are estimated, we can extract the local normal patterns based descriptor from them. This descriptor follows the encoding rule like this. First, for each encoded pixel, a neighbor area is defined as a set of sampling points forming a circle centered at the encoded pixel. The neighbor area is usually classified with $Q_{r,p}$, which denotes the parameters of this cod-

ing that r is the radius of the circle and p is the amount of sampling points. Second, we compare the curvature of encoded point C_p to the curvature of each sampling point C_{Samp}. We temporarily encode the sampling point with 0 when $C_p > S_{Samp}$, or encode it with 1 if $C_p \leq C_{Samp}$. Third, connecting these binary codes starting from the top-left in the clockwise direction, we obtain the binary number. Then it is converted to the decimal number which is set as the label of encoded pixel. The labels which result from such a process are referred to as the local normal patterns (LNP).

The principal curvatures based LNP map achieved above is further divided into several local patches. Then extracting the patch based LNP histograms H and concatenating them to form a large histogram G. Finally, each original facial surface is described by three LNP histograms $G_{\lambda_1}, G_{\lambda_2}$ and G_{λ_3} associated to three principal curvatures.

3.5. W-SRC and fusion

Weighted sparse representation-based classifier (W-SRC) applied in this paper is following the presentation of Li *et al.*s work in [11] which demonstrated in particular that solving W-SRC amounts to computing a single SRC with global feature vectors in stacking the weighted feature vectors of each patch and can also be solved by the OMP algorithm [17]. The minimal weighted reconstruction residual r_i, the matching score calculated by W-SRC, can be used to determine the similarity between two face surfaces LNP histogram associated to the principal curvatures.

Therefore, for a query image, $3 \times n$ sets of weighted reconstruction residual can be computed corresponding to three principal curvatures generated with n sequences of Borel subsets. Considering that three principal curvatures with the same Borel subset B_i can provide much geometric information mutually complementary, the matching scores $r_{\lambda_1}, r_{\lambda_2}, r_{\lambda_3}$ obtained corresponding to them need to be fused and generate fusion matching score r_{B_i} in dynamic fusion method [6]. According to the minimal r_{B_i}, the identified candidate of Borel subset B_i is confirmed. Then the gallery face image that hold the maximal vote amount of candidate and maximal matching score r_{B_i} is declared as the identity of the query image.

4. Experiments

In this section, we introduce the database and describe its particularities. Then we present our experiment settings and show the experiment results that indicate the third new principal curvature containing meaningful geometric information and improving the recognition performance.

4.1. Database

The FRGC v2.0 database [2] is made up of 4007 textured 3D face scans of 466 subjects with different facial expressions. The face scans are captured in controlled lighting and pose by the Minolta Vivid 900 scanner. FRGC v2.0 is the largest public 3D face database in the literature and has become the benchmark for evaluating 3D FR approaches. In the experiment, we take the earliest image of each person to group the gallery set (466 images) and the rest form the probe gallery (3541 images).

4.2. Experiment settings

The purposes of our experiment are to examine the recognition efficiency of the third principal curvature estimated from asymptotic cones and to demonstrate that different scale of Borel subset of asymptotic cones can offer complementary information in the recognition process.

As the presentation above, the principal curvatures are affected by the change of radius of the Borel subset around the vertex. Therefore, we build three sets of experiments corresponding to 3 Borel subsets scales: geodesic radius 3, 5, 7. Only the vertices in this Borel subset support the estimation of principal curvatures.

With each scale of Borel subset, we get three curvature faces. To highlight the discriminative power of the third principal curvature, we take two score level fusions, the first fusion is between the first and second principal curvatures (Fusion $\lambda_1 + \lambda_2$) and the second fusion is participated by all of three principal curvatures (Fusion $\lambda_1 + \lambda_2 + \lambda_3$). Finally, the fusion with voting between different Borel subset scales is presented.

As described in section 3.4, the curvature face is separated into 12×10 patches to highlight local geometric feature. Following this setting, each patch contains sufficient vertices (around 800) to generating the descriptor of patch and the descriptor of image wont be too large to increase the time complexity. The parameters of LNP are set as $Q_{2,16}$ referring to the experiment result in [11].

4.3. Experiment results

We test the discriminative power of each principal curvature based LNP descriptor in each scale and their combinations as displayed in Table. 1

From the Table 1, we observe that the rank-1 recognition rate of each principal curvature based descriptor is around 85%. As we discuss in section 3.2, each principal curvature can provide sufficient geometric information for the LNP descriptor, even the principal curvature λ_3, who provides the recognition rate is a little lower than the other two principal curvature, which is ignored in other related curvature-based work. In a further step, we take the fusion of λ_1, λ_2 and $\lambda_1, \lambda_2, \lambda_3$, and the rank-1 recognition rate is displayed in the 4th and 5th row in the Table 1 that the result fused of 3 curvatures is around 90% which is higher than the ones with one curvature or the ones with first two curvatures. This result indicates that each three principal curvatures are mean-

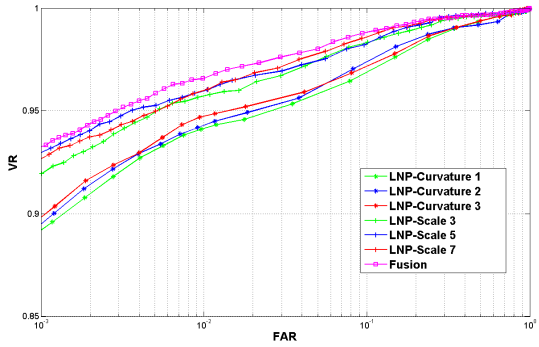

Figure 4. Receiver operating characteristic (ROC) curves between FAR and VR of our proposed method

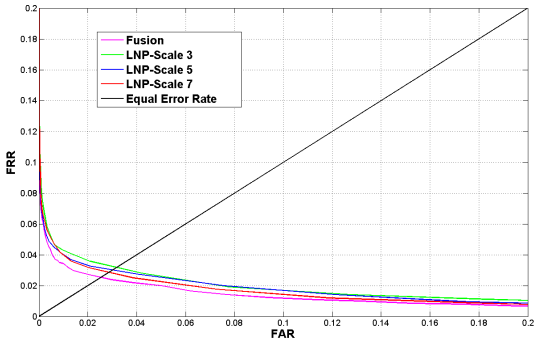

Figure 5. ROC curve between FAR and False Reject Rate (FRR) of our proposed method

Scale of Borel subset	Radius 3 (%)	Radius 5 (%)	Radius 7 (%)	Scale realtated Fusion (%)
λ_1	85.82	85.87	85.70	90.30
λ_2	85.87	85.48	85.33	89.99
λ_3	83.06	85.39	84.46	89.70
$\lambda_1 + \lambda_2$	89.42	89.56	88.79	92.23
$\lambda_1 + \lambda_2 + \lambda_3$	90.72	90.72	90.50	**93.16**

Table 1. Rank-1 identification rate of each principal curvature related descriptor and the fusion

Approaches	Year	Rank-1 Score	Verification Rate
Kakadiaris *et al.*[10]	2007	97.00%	97.30%
Wang *et al.* [25]	2010	98.30%	97.97%
Spreeuwers [20]	2011	99.00%	94.60%
Ballihi *et al.* [1]	2012	98.20%	-
Huang *et al.* [5]	2012	97.6%	98.4%
Li *et al.* [12]	2013	96.30%	-
Smeets *et al.* [19]	2013	89.60%	79.00%
Proposed Method	2014	93.16%	93.33%

Table 2. Performance comparison on FRGC v2.0 database

ingful in the face recognition based on mesh model and they can offer mutual complementary geometric information to improve the recognition performance.

The first three rows in the table 1 present the recognition rate of the principal curvature is influenced slightly by the variety of Borel subsets scale. But the recognition rate of fusion between different scales is improved indeed from 85% to 90% which shows the descriptors in different scales display discrepant properties of the local surface and if combine them together the recognition rate could be 93.16%.

We also performed the experiments in the scenario of verification with 2 modalities, i.e., fusion of three principal curvatures in single scale and fusion of three principal curvatures and three scales. For each subject, the first image was regarded as the gallery and the remaining images are treated as the probe to calculation the verification rate (VR) at the false acceptance rate (FAR) and the equal error rate (EER). The experiment result is shown in Fig.5, from which we can draw similar conclusion as in identification. We highlight the result of fusion of all the three principal curvatures and three scales that VR is 93.33% at FAR is 0.001 and VR is 96.57% at FAR is 0.01 and EER is 2.56%.

Moreover, we compare our result with other algorithms that have been published and validated on the same space in Table 2. As we presented in section 1, the maximal curvature and the minimal curvature are used in [10, 25, 12] to describe the local surface geometric property and build the descriptor. The result shows that some other methods perform better, while some perform worse. Although the recognition result of our proposed method is not the best, our experiments have demonstrated that the isolated third principal curvature estimated by asymptotic cones has discriminative power and it can offer the complementary local surface geometric information to improve the recognition performance. In addition, the result of the experiment about the fusion of descriptor with different scales also demonstrates the three multi-scale principal curvature based descriptor carry mutual complementary information. The third novel local surface geometric descriptor fitting to the mesh model may also be adopted in the methods mentioned above to ameliorate the curvature based facial descriptor.

5. Conclusion

This paper proposed a novel local facial surface descriptor based on three principal curvatures estimated by asymptotic cones which fit better the case of triangulation mesh model. The asymptotic cone is an important extension of the asymptotic direction to the mesh model and permits to generate three principal curvatures describing the geometric property of each vertex. The experiment on FRGC v2.0 shows that the third principal curvature carrying supplementary geometric information could improve the recognition performance and the fusion could combine the geometric details to describe the local surface more precisely and accurately.

In the further work, we will analyze the properties and function of the eigenvector corresponding to the eigenvalue on each vertex. And the combination of the eigenvector and eigenvalue may provide more powerful surface descriptor

for face recognition.

Acknowledgment

This work was supported in part by the French Research Agency, l'Agence Nationale de Recherche (ANR), through the projects Biofence and Jemime, under the grants ANR-13-INSE-0004-02 and ANR-13-CORD-0004-02; the National Natural Science Foundation of China (NSFC) under Grant 61202237; the Specialized Research Fund for the Doctoral Program of Higher Education (20121102120016); the joint project by the LIA 2MCSI laboratory between the group of Ecoles Centrales and Beihang University; and the Fundamental Research Funds for the Central Universities.

References

[1] L. Ballihi, B. Ben Amor, M. Daoudi, A. Srivastava, and D. Aboutajdine. Boosting 3-d-geometric features for efficient face recognition and gender classification. *Information Forensics and Security, IEEE Trans. on*, 7(6):1766–1779, 2012.

[2] K. W. Bowyer, K. Chang, and P. Flynn. A survey of approaches and challenges in 3d and multi-modal 3d + 2d face recognition. *Computer vision and image understanding*, 101(1):1–15, 2006.

[3] D. Cohen-Steiner and J.-M. Morvan. Restricted delaunay triangulations and normal cycle. In *Proceedings of the nineteenth annual symposium on Computational geometry*, pages 312–321. ACM, 2003.

[4] D. Cohen-Steiner, J.-M. Morvan, et al. Second fundamental measure of geometric sets and local approximation of curvatures. *Journal of Differential Geometry*, 74(3):363–394, 2006.

[5] D. Huang, M. Ardabilian, Y. Wang, and L. Chen. 3-d face recognition using elbp-based facial description and local feature hybrid matching. *Information Forensics and Security, IEEE Trans. on*, 7(5):1551–1565, 2012.

[6] D. Huang, Y. Tang, Y. Wang, L. Chen, and Y. Wang. Hand-dorsa vein recognition by matching local features of multisource keypoints. *IEEE Trans. on Cybernetics*, 2014.

[7] W. Hwang, X. Huang, K. Noh, and J. Kim. Face recognition system using extended curvature gabor classifier bunch for low-resolution face image. In *Computer Vision and Pattern Recognition Workshops (CVPRW), IEEE Computer Society Conference on*. IEEE, 2011.

[8] A. Jain, L. Hong, and S. Pankanti. Biometric identification. *Communications of the ACM*, 43(2):90–98, 2000.

[9] A. K. Jain, A. Ross, and S. Prabhakar. An introduction to biometric recognition. *Circuits and Systems for Video Technology*, 14(1):4–20, 2004.

[10] I. A. Kakadiaris, G. Passalis, G. Toderici, M. N. Murtuza, Y. Lu, N. Karampatziakis, and T. Theoharis. Three-dimensional face recognition in the presence of facial expressions: An annotated deformable model approach. *Pattern Analysis and Machine Intelligence, IEEE Trans. on*, 29(4):640–649, 2007.

[11] H. Li, D. Huang, J.-M. Morvan, L. Chen, and Y. Wang. Expression-robust 3d face recognition via weighted sparse representation of multi-scale and multi-component local normal patterns. *Neurocomputing*, 133:179–193, 2014.

[12] H. Li, D. Huang, J.-M. Morvan, Y. Wang, and L. Chen. Towards 3d face recognition in the real: A registration-free approach using fine-grained matching of 3d keypoint descriptors. *International Journal of Computer Vision*, 2014.

[13] C. Maes, T. Fabry, J. Keustermans, D. Smeets, P. Suetens, and D. Vandermeulen. Feature detection on 3d face surfaces for pose normalisation and recognition. In *Biometrics: Theory Applications and Systems, IEEE International Conference on*, pages 1–6. IEEE, 2010.

[14] J.-M. Morvan. *Generalized curvatures*. Springer, 2008.

[15] J.-M. Morvan and B. Thibert. On the approximation of a smooth surface with a triangulated mesh. *Computational Geometry*, 23(3):337–352, 2002.

[16] J.-M. Morvan and B. Thibert. Approximation of the normal vector field and the area of a smooth surface. *Discrete & Computational Geometry*, 32(3):383–400, 2004.

[17] Y. C. Pati, R. Rezaiifar, and P. Krishnaprasad. Orthogonal matching pursuit: Recursive function approximation with applications to wavelet decomposition. In *Signals, Systems and Computers, Asilomar Conference on*. IEEE, 1993.

[18] P. J. Phillips, P. J. Flynn, T. Scruggs, K. W. Bowyer, J. Chang, K. Hoffman, J. Marques, J. Min, and W. Worek. Overview of the face recognition grand challenge. In *Computer vision and pattern recognition, IEEE Computer Society Conference on,*. IEEE, 2005.

[19] D. Smeets, J. Keustermans, D. Vandermeulen, and P. Suetens. meshsift: Local surface features for 3d face recognition under expression variations and partial data. *Computer Vision and Image Understanding*, 117(2):158–169, 2013.

[20] L. Spreeuwers. Fast and accurate 3d face recognition. *International Journal of Computer Vision*, 93(3):389–414, 2011.

[21] X. Sun and J.-M. Morvan. Asymptotic cones of embedded singular spaces, submitted.

[22] X. Sun and J.-M. Morvan. Curvature measures, normal cycles and asymptotic cones. page 3, 2013.

[23] P. Szeptycki, M. Ardabilian, and L. Chen. A coarse-to-fine curvature analysis-based rotation invariant 3d face landmarking. In *Biometrics: Theory, Applications, and Systems. IEEE International Conference on*. IEEE, 2009.

[24] K. Tonchev, A. Manolova, and I. Paliy. Comparative analysis of 3d face recognition algorithms using range image and curvature-based representations. In *Intelligent Data Acquisition and Advanced Computing Systems (IDAACS), IEEE International Conference on*. IEEE, 2013.

[25] Y. Wang, J. Liu, and X. Tang. Robust 3d face recognition by local shape difference boosting. *Pattern Analysis and Machine Intelligence, IEEE Trans. on*, 32(10):1858–1870, 2010.